Original Research Article

First principles Investigation of Structure and electronic properties of $NiTe_2$ Fermi Crossing Type-II Dirac Semimetal.

Abstract

Electronic structure aspect of Transition metal dichalcogenides (TMDs) have so far received intensive research interest. $NiTe_2$ is a noble candidate for type-II DSM with Dirac point near the Fermi surface. In this paper structure and electronic properties are studied using density functional theory (DFT) calculations. The density of states, the partial density of states and band structure calculations are performed. $NiTe_2$ is projected to be a promising candidate for exploring topological superconductivity. From the result obtained in our work the valence bands cross the fermi surface which is the greatest indicator that the material been studied is purely semimetal with Dirac point close to the fermi level as can be observed from the bands structure plot. It is also worthy to note that the contribution of the Ni and Te orbitals are also discussed based on the partial density of states plots. Lastly our calculations revealed the existence of Dirac type-II point in $NiTe_2$. Our work provides a way for studying further the optoelectronic properties of $NiTe_2$ in the field of spintronics and infrared plasmonics.

Keywords: DFT, Structure properties, Dirac semimetal, $NiTe_2$

1.0 Introduction

The combination of nickel and telluride in the Ni-chalcogenides family are the very few being perceived due to the nature of tellurium that is comparatively denser than both Selenium and Sulphur, thus poorly adhesive onto the substrate [1]. Nguyen et al. studied the structure of liquid $NiTe_2$ by using the technique of neutron diffraction [2]. Lately 2D materials have captured a great deal of study focused particularly because of their separate physical properties and ability to fulfilled the future demands of the nano-electronic industry on adaptability, multi-functionality

and flexibility. During the course of investigating for expected promising materials, layered transition metal di-chalcogenides have been important members of the 2D materials [3]

Immediately after the discovery of 3D Dirac semimetals (DSMs), which are regarded as type-II fermions in which the Dirac node is enclosed by an electron pocket, has generated a huge research interest because of the rich physics involve and the tremendous applications therein. Recently the attention has been shifted partially to the so called type-II Dirac semimetals where the Dirac cone is strongly tilted because of the broken Lorentz symmetry, and due to that the Dirac point appears only at the contact of hole and electron pockets [4-5]. Transition metal di-chalcogenides offer a perfect platform to experimentally understand Dirac fermions. Though, usually these interesting quasiparticles are situated far-away from the Fermi level, restraining the contribution of Dirac-like carriers to the transport properties. $NiTe_2$ accommodates both bulk Type-II Dirac points and topological surface states [6]. Type-II Dirac semimetals also called Weyl semimetals are characterized by strongly tilted Dirac cones in a way that Dirac the Dirac node emerges at the boundary of electron and hole pockets as a new state of Quantum matter, different from the standard Weyl points with a point like Fermi surface which are called as type-I nodes. The type-II Dirac semimetals were recently predicted by theory and have since been confirmed experimentally in some other transition metal di-chalcogenides [7]. Even recently, many transition metal di-chalcogenide materials, comprising of PtTe2, PdTe2 and PtSe2, were predicted and found to display tilted Dirac cones close to their Fermi surface. For these considered Dirac type-II compounds, the Hamiltonian comprises of the type-I linear Hamiltonian and an additional, momentum dependent, term that breaks Lorentz invariance and leads to quasiparticles showing a momentum energy relation that depends on the direction of travel [8]. New quantum phenomena like planar Hall effect, and superconductivity have been theoretically projected and experimentally confirmed in bulk NiTe2 [9]. Most of the transition metal di-chalcogenides can achieve superconductivity by pressure or doping. Investigation on the pressure resistant impression on resistant behavior of NiTe2. NiTe2 shows metallic property at ambient pressure in temperature ranging from 2000-3000000 [10].

Recent studies proposed to find experimental evidence for its existence through the mapping of its electronic band structure via angle-resolved-photoemission spectroscopy (ARPES) measurement or extracting its Berry phase from magnetization measurements [11-12]. Though, comprehensive information about the fermi surface topography, extracted from the angular dependence of the quantum oscillations, along with a comparison with density functional theory calculations are still lacking.

Our intention in this work is to investigate on the crystal structure and electronic properties of $NiTe_2$ as a Fermi crossing Dirac type-II semimetal candidate.

2.0 Method of calculation

Theoretically discourse Schrodinger Equation is a quantum mechanical idea that provides the exact manners and behavior of system's natural states like particle motion and its wave-function. Electronic structure of any system can be precisely fortified using the solution of SE without any empirical or semi-empirical parameters [13-14]. Though, Schrodinger equation is not easy to solve because of the nucleus-electron interaction, thereafter a solution was suggested by prominent Born-Oppenheimer approximation. Earlier scholars assume that to split electronic coordinates and nuclear from many-body wave function, the nuclei must be assessed adiabatically because of the variation in mass between electron and nuclei [15]. Even though with this clarification and simplification yet, many-body problem remains enormously problematic to work out. Then via the Hartree-Fock (H-F) approximation many body-problem can be simplified to a single-electron problem and offer an exact description of electron exchange, sadly it did not describe the electronic correlation [16]. Because of the fact that, it is not possible to solve Schrodinger equation for N-electron, in the year 1964 density functional theory (DFT) was introduced by the renowned Hohenberg and Kohn as a technique to offers the description of the electronic structure of a system at ground state with idea stated that all ground sate properties for many-systems are functional of the electronic density [17-18]. The minimum value of the total energy functional is the definite single electron ground state density [19]. Kohn and Sham suggested an equation that succeeded in replacing the problem of mutually interacting

electrons in an external ion potential to an equivalent set of self-consistent one electron [20]. The significance of electron-electron interaction is provided by Generalized Gradient Approximation (GGA) [21] OR Local Density Approximation (LDA) [22]. Computations based on density functional theory are well-known and distinguished from other ab initio methods as first principle calculations with an approximate error of 10^{-3} eV, the errors can be significantly minimized by adjusting the K-points mesh or the cutoff energy. In numerous cases, the first principles calculations within the of density functional theory framework offers exact guesses of many properties of materials, stable configuration and total energy.

In this work, we perform the first principles calculations using the Plane-Wave Self-consistent field (PWSCF) program of the Quantum Espresso code [23] based on the density functional theory (DFT). A cut off energy for the wavefunction is taken to be 150 Ry. K-point grid in the Brillouin zone is set by 8 × 8 × 1 grid for $NiTe_2$ in the Monkhorst-Pack method. [24]. The Generalized Gradient Approximation (GGA) of Perdew-Burke-Ernzerhof (PBE) formalism is adopted for the exchange correlation potential (Xc) [25] and is used for discussing the electronic properties of the material. To obtain optimized atomic configurations of $NiTe_2$, variable cell relaxations for atomic coordinates and dimension of the cell using intrinsic Broyden-Fletcher-Gold farb-Shanno (BFGS) algorithm were performed. Fig. 1 display the relax structure of $NiTe_2$. The model are considered as optimized structure when the Hellmann-Feynman forces and all components of the stress are less than 0.0005 Ry/a.u respectively.

3.0 Results and Discussions.

3.1 Structural parameters

The complete relaxation calculations were initially performed to determine the accurate internal positions of the atoms. All atomic positions and lattice parameters were optimized. Numerical calculation was implemented in Quantum ESPRESSO simulation package.

The calculated lattice parameters, Fermi energy, density and volume for the relaxed structure of $NiTe_2$ are given in the table below. It is worth noting that our calculations result are in good agreement with experimental data. Ni and Te consist of stacked Te-Ni-Te layers, where the metal Ni atom is coordinated octahedrally with six atoms of Te. The atoms are covalently bonded within one layer, while the sandwich layers are coupled only by weak Vander Waals interaction [26]. Also using the Birch-Murnaghan equation of state given by Equ. (1) below the optimization of the relaxed structure of $NiTe_2$ was carried out by GGA-PBE to compute the ground state properties which consist of the bulk modulus B_o and the the first derivative of the modulus B' [27].

$$E(v) = E_o + \left\{ \left[\left(\frac{V_o}{V} \right)^{\frac{2}{3}} - 1 \right]^2 \left[(6-4) \left(\frac{V_o}{V} \right)^{\frac{2}{3}} \right] + \left[\left(\frac{V_o}{V} \right)^{\frac{2}{3}} - 1 \right]^3 B' \right\} \left(\frac{9 V_o B_o}{16} \right) \qquad (1)$$

Where Eo and Vo are minimum equilibrium energy and volume respectively. Where Fig. 1 depicts the optimization plots using GGA. For GGA we found that the lowest equilibrium energy value is -157.6 Ry corresponding to 500.4 $(a.u)^3$. Cohesive energy is the work which is required when a solid is decomposed into a free isolated atom, the more negative the cohesive energy, the more stable the material, the expression of the cohesive energy is given in the equation below

$$E_{coh}^{NiTe_2} = \frac{E_{solid}^{NiTe_2} - Z \times (aE_{atom}^{Ni} + bE_{atom}^{Te_2})}{Z \times (a+b)} \qquad (2)$$

Where Z is the number of $NiTe_2$ per unit cell. In order to get the structural parameters, such as the equilibrium lattice parameters a, c, the bulk modulus B_o and its pressure first derivative B', we have computed the cohesive energy in Equation for $NiTe_2$. The cohesive energy as a function

of volume are fitted with Birch Murnaghan's first equation of state (EOS). The obtained cohesive energy against the volume data for $NiTe_2$ are shown graphically in Figure.

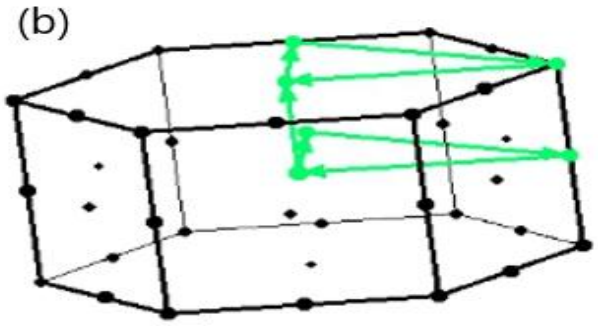

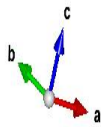

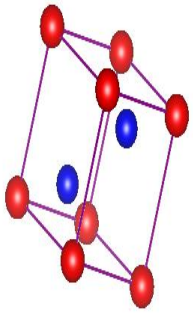

Fig. 1(b) VESTA view of $NiTe_2$

Fig. 1(a) first Brillouin zone of $NiTe_2$ from XCRYSDEN

3.2 Electronic Properties

The most important characteristics of a type-II Dirac semimetal is the tilted 3D Dirac cone in the band structure. Electronic band structure calculation is very important for describing the behavior of materials. Analysis of band structure, the total density of states (TDOS) and partial density of states (PDOS) of $NiTe_2$ were performed. The electronic band structure of $NiTe_2$ were calculated within PBE approximation based on first principles calculations. From our band structure calculations, the Fermi level lies at 0 eV. The valence band were found to lie above the Fermi level, hence the material is said to behave as Dirac type-II semimetal.

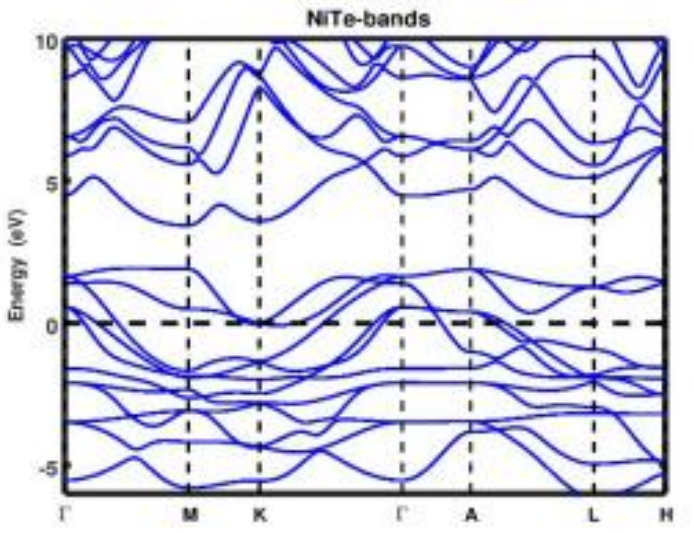

Fig. 2. electronic band structure of $NiTe_2$. Dirac type-II is observed along Gamma to H direction with the node located above the Fermi level. This node is located slightly above 100 meV in the Quantum Espresso [23] implementation of density functional theory (DFT). The valence bands crosses Ef. The electronic structure of $NiTe_2$ displays strong 3-dimensionality, exhibited from the different band structures on the high symmetry K-points.

Table 1: Calculated equilibrium lattice parameter, volume, density, minimum energy E_0, and the enthalpy of formation of $NiTe_2$

	a $= b\ (Å)$	$c(Å)$	$V\ (Å)^3$	ρ (g/cm^3)	E_0 (Ry)	H (Ry)	B(Gpa) B’
This work	3.7925	5.9395	73.98365	7.01381	-157.58461	-396.22229 1.00	224.6
Experiment [28]	3.899	5.243	69.036	7.550			

We have also calculated and analyzed the total density of states (TDOS) and partial density of states (PDOS) for NiTe2 as can be seen in Fig. 3(a) and (b) along with the fermi energy level represented by a pin dash. DOS aid to the elaboration of the nature of the bandgap and PDOS provides details information about the origin of bands for both valence and conduction bands. In the total density of states plot, near the fermi level i.e at 0 eV there are available states which also shows that the studied material is behaving as a Dirac type-II semimetal. The TDOS confirms that the bands near the fermi level, Ef, are dominated by Te p-orbital. Ni d-orbital derived bands appear away from the Fermi level.

To show the thermodynamic stability of our material we calculated the enthalpy of formation H using the following Equ. (2)

$$H = \frac{(E_T(NiTe_2) - mE_{Ni} - gE_{Te})}{(m+g)} \qquad (2)$$

Where the term $E_T(NiTe_2)$ is the total ground state energy of the material been studied and E_{Ni} and E_{Te} are the ground state energies of the Ni and Te in the unit cell respectively. The parameters m and g in the equation represent the number of the individual atoms in the unit cell. In this work, we reformed Equ. (2) above for application on $NiTe_2$ Fermi Dirac type-II material for GGA-PBE as shown.

$$H = \frac{E_T^{GGA}(NiTe2) - (mE_{Ni}^{GGA} - gE_{Te}^{GGA})}{(m+g)} \qquad (3)$$

For a material to be stable, its total energy must be lower than the sum of energies of its components [29]. Consequently, the negative value obtained for the enthalpy of formation as presented in Table 1 confirms that the studied material is stable

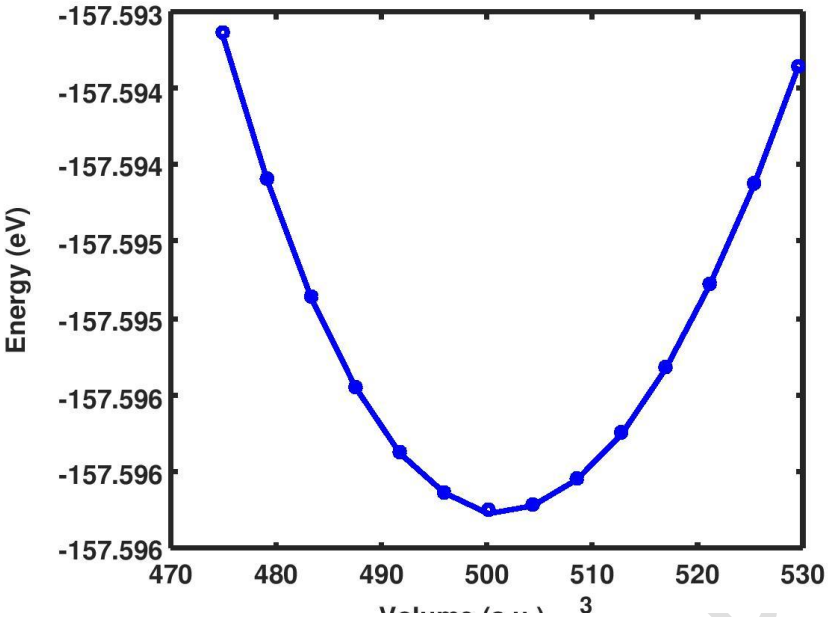
-157.593
-157.594
-157.594
-157.595
-157.595
-157.596
-157.596
-157.596
Energy (eV)
470
480
490
500
510
520
530

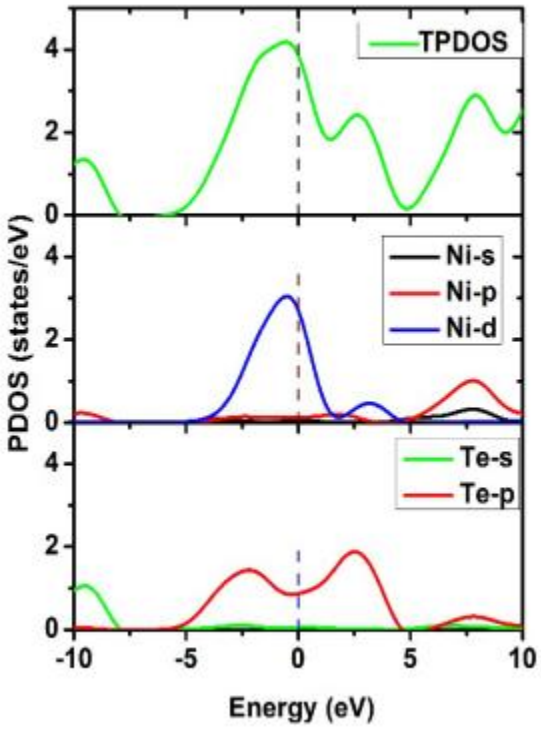
TPDOS
Ni-s
Ni-p
Ni-d
Te-s
Te-p
PDOS (states/eV)
Energy (eV)

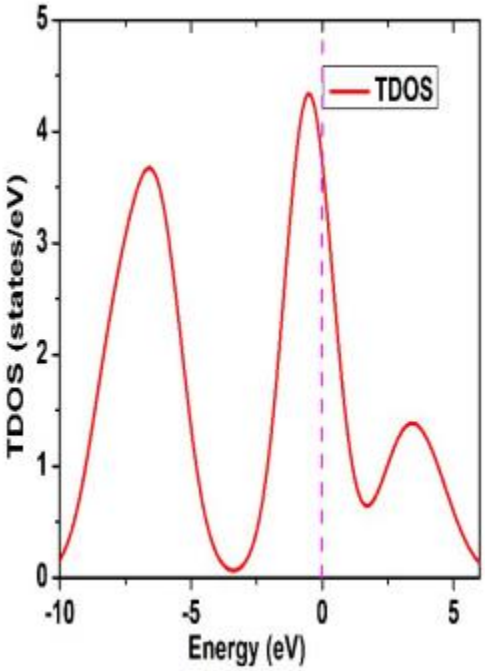
TDOS
TDOS (states/eV)
Energy (eV)

Fig 3: Calculated and analyzed the total density of states (TDOS) and partial density of states (PDOS) for NiTe2

Fig. 3 (b) shows the total partial density of states (TPDOS) for $NiTe_2$ and the contribution of each of the individual orbitals of Ni and Te. Ni d-orbital contributed significantly in the conduction band and the p-orbital contributed also significantly in the valence band. While the p-orbital of Te contributed more in both the valence and conduction bands.

4.0 Conclusions

In this work, structure and electronic properties of $NiTe_2$ Fermi crossing type-II Dirac semimetal where studied using first principles calculations. A reasonable agreement between calculated lattice parameters and experimental data was obtained for GGA-PBE pseudopotential method. Our calculation indicate that $NiTe_2$ is type-II DSM with Dirac point near the Fermi surface. We predict that $NiTe_2$ is a noble candidate for type-II DSM. Our work establishes $NiTe_2$ as a major candidate for exploration of Dirac Fermions and applications in transition metal dichalcogenides based infrared plasmonics, spintronic devices and ultrafast optoelectronics.

References

1. Anand, T.J.S.; Zaidan, M., Azam, M.A. et al. Structural studies of NiTe2 thin films with the influence of amino additives. Int J Mech Mater Eng 9, 18 (2014).
2. V T Nguyen1, M Gay1, J E Enderby1, R J Newport1 and R A Howei. The structure and electrical properties of liquid semiconductors.
3. Qianwen, W.; Ping, W.; Gengyu, C.; Min, H. First Principle Study of the Structural and Electronic Properties of MoS2-MoTe2 Monolayer Heterostructures. J. Phys. D: Appl. Phys. 46 (2013) 505308 (7pp).
4. Burkov, A. A. Topological Semi-metals. Nat. mater. 2016,15, 1145-1148.
5. Soluyanov, A. A.; Gresch, D.; Wang, Z.; Wu, Q.; Troyer, M.; Dai, X.; Bernevig, B. A. Type-II Weyl Se-metals. Nature 2015, 527, 495-498.
6. Saumya, M.; Sophie, F.; Pabitra, K.; Timur, K.; Laurent, C.; Mathew, D.; Jeffrey, B. Fermi-crossing Type-II Dirac Fermions and Topological surface states in NiTe2. Scientific Reports, 2020, 10, 12957.
7. Chungian , X.; Bin, L.; Wenhe, J.; Wei, Z.; Bin, Q.; Raman, S.; Nikolai, D.; Zhigalo, Yanpeng, Q.; Fang-Cheng, C.; Xiaofeng, X. Topological Type-II Dirac Fermions Approaching the Fermi Level in a Transition Metal Dichalcogenide NiTe2. Chem. Mater. 2018, 14, 4823-4830
8. Huang, H.; Zhou, S.; Duan, W. Phys. Rev. B 94, 121117®, 2016.
9. Zheng, F. P.; Li, X.-B.; Tan, P.; Lin, Y. P.; Xiong, L. X.; Chen, X. B.; Feng, J. Emergent Superconductivity in Two Dimensional NiTe2 Crystals. Phys. Rev. B 2020, 101, 100505(R).
10. Tao, L.; Ke, W.; Chungiang, X.; Qian, H.; Hao, W.; Jun-Yi, G.; Shixun, C.; Jincang, Z.; Wei, R.; Xiaonfeng, X.; Nai-chang, Y.; Bin, C.; Zhenjie, F. Pressure-Induced Superconductivity in topological type-II Dirac semimetal NiTe2. Cond-Mat. Supr-Con. 2019.
11. Ghosh, B.; Mondal, D.; Kuo, C. N.; Lue, C. S.; Nayak, J.; Fujii, J.; Vobomik, I.; Politano, A.; Agarwala, A. phys. Rev. B 100, 2019, 195134.
12. Xu, C.; Li, B.; Jiao, W.; Zhou, W.; Qian, B.; Sankar, R.; Zhigalo, N. D.; Qi, Y.; Qian, D.; Chou, F. C.; Xu, X. Chem. Mater. 30, 2018, 4823.

13. Foresman J, Frisch A. Exploring Chemistry with Electronic Structure Methods 2nd ed. Gaussian, Inc, Pittsburgh, PA.

14. Novak P, Boucher F, Gressier P, Blaha P, Schwarz K. Phys. Rev. B 63 (2001) 235114-1–8.

15. Filippov A, Non-linear Non-local Schrodinger equation in the contest of quantum mechanics. Phys. Lett A 1996; 215:32-9.

16. Callaway J, March N. Density Functional Methods: theory and application solid state physics. 1984; 38:135-221.

17. Kuznetsov A, Medvedev I. Does really Born-Oppenheimer Approximation Break Down in Charge Transfer Process? An Exactly Solvable Model. Chem. Phys. 2006; 324:148-59.

18. Chaikin P, Lubensky T. principles of Condensed Matter Physics. Cambridge Univ. Press; 2000.

19. Hohenberg P, Kohn W. Density Functional Theory. Phys. Rev. B 194; 136:864-76.

20. Dreizler R, Gross E. Density Functional Theory: An Approach to the Quantum Many-Body Problem. Springer Science & Business Media; 2012.

21. Payne M, Teter M, Allan D, Arias T, Joannopoulos J. Iterative Minimization Techniques for Ab Initio Total Energy Calculations Molecular Dynamics and Conjugate Gradients. Rev. Modern Phys. 1992; 64:1045.

22. Kohn W, Sham LJ. Self-Consistent Equations Including Exchange and Correlation Effects. Phys. Rev. 1965; 140:A1133.

23. Giannozzi, P.; Baroni, S.; Bonini, N.; Calandra, R.; Cavazzoni, C.; Caresoli, D.; Chiarotti, G.L.; Cococcioni, M.; Dabo, I. Jorn. Phys. Condens. Matter 21, 2009, 395502.

24. Monkhorst, H. J.; Pack, J. D. special points for Brillouin zone integrations. Phys. Rev. B 13, 12, 1976, 5188.

25. Perdew, J. P.; Burke, K.; Ernzerhof, M. Phys. Rev. Lett. 1996, 77, 3865-3868.

26. Hartwigsen, S. Goedecker, J. Hutter, Relativistic separable dual-space Gaussian pseudopotentials from H to Rn, Phys. Rev. B 58,1998, 3641.

27. Birch, F. Finite elastic strain of cubic crystal. Phys. Rev. 71. 1947. 809-824.

28. Jain, A.; Ong S. P.; Hautier, G.; Chen, W.; Richards, W. D.; Decek, S.; Cholia, S.; Gunter, D.; Skinner, D.; Ceder, G.; Pearson, K. A. The Materials Project: A material genome approach to accelerating materials innovation APL Materials, 2013, 1(1), 011002.
29. Wu, S.; Fecher, G. H.; Shabab, S.; Felser, C. Elastic properties and stability of Heusler Compounds: cubic Co 2 YZ compounds with L 2 1 structure. J. Appl. Phys. 125 (2019).
30. Kudo, K.; Ishii, H.; Nohara, M. Composition-Induced Structural Instability and Strong-coupling Superconductivity In Au1-xPdxTe2 Phys. Rev. B 93 140505.